Trajectory of Nucleosomal Linker DNA Studied by Fluorescence Resonance Energy Transfer

Katalin Tóth,* Nathalie Brun, and Jörg Langowski

Division of Biophysics of Macromolecules (H0500), Deutsches Krebsforschungszentrum,
Im Neuenheimer Feld 280, D-69120 Heidelberg, Germany

ABSTRACT: While the structure of the nucleosome core is known in atomic detail, the precise geometry of the DNA beyond the core particle is still unknown. We have used fluorescence resonance energy transfer (FRET) for determining the end-to-end distance of DNA fragments assembled with histones into nucleosomes. The DNA of a length of 150−220 bp was labeled with rhodamine-X on one end and fluorescein or Alexa 488 on the other. Assembling nucleosomes on these DNA fragments leads to a measurable energy transfer. The end-to-end distance computed from the FRET increases from 60 ± 5 Å at 150 bp to 75 ± 5 Å at 170 bp without measurable change above it. These distances are compatible with different geometries of the linker DNA, all having in common that no crossing can be observed up to 220 bp. Addition of H1 histone leads to an increase in energy transfer, indicating a compaction of the linker DNA toward the nucleosome.

The packing of the DNA into chromosomes in the eukaryotic cell has been an unresolved puzzle for many years. At the lowest level of compaction, DNA is bound to histones into nucleosomes (*1*, *2*). This structure is quite well understood: about two turns of DNA are wrapped around the histone octamer core, one histone octamer and 146 bp of DNA form a biochemically stable unit called the core particle, and the spacing between successive nucleosomes is 160−220 bp depending on the cell type and species. The crystal structures of the histone octamer (*3*) and of the full nucleosome core particle (*4*) have been solved at atomic resolution.

However, at the next higher level of packing, the situation is much less clear. Electron microscopic images of chromatin preparations typically present a 10 nm thick fiber in hypotonic conditions and a "30 nm fiber" under preparation conditions corresponding to the physiological environment. A variety of concurrent models have been proposed to explain the folding of the nucleosome chain into the 30 nm fiber, e.g., the solenoid model where the DNA follows a continuous spiral path (*5*), or "zigzag" models, where the linker DNA is straight (*6*, *7*). The detailed structure of such models depends critically on the geometry of the DNA beyond its direct contact with the nucleosome. Open questions are whether the linker arms cross after leaving the core, whether they bend between two nucleosomes or are straight, and what angle they enclose under various buffer conditions. The question whether the linker DNA arms cross each other in the actual chromatin structure is at the center of the so-called *linking number paradox*. From a recent analysis (*8*) it appears that the observation that the binding of each nucleosome to a circular DNA produces a linking number difference of $\Delta Lk = -1$, instead of -2 as would be expected

for two superhelical turns per nucleosome, can be explained by the assumption that the linker DNA arms do not cross.

Studies on oligonucleosomes can help to decide about the linker DNA geometry. Ultracentrifugation and light scattering studies on di- and trinucleosomes in solution were interpreted via hydrodynamic models. It was shown that the internucleosomal distance decreases with salt concentration in the 5−20 mM NaCl region, suggesting a bending of the linker DNA (*9*, *10*). Our recent neutron small angle scattering data obtained on di- and trinucleosomes indicate a further compaction up to 100 mM NaCl, even in the absence of linker histone (*11*). Cryoelectron microscopy results suggest that the entry−exit angle of the linker arms decreases from 100° at 5 mM NaCl to 45° at 20 mM, without further change at higher salt concentration (*12*, *13*). From scanning force microscopy images it was proposed that removal of linker histones or the H3 tail doubles the distance between the nucleosomes in the chromatin fiber, without significantly changing the entry−exit angle of $100 \pm 40°$ (*14*).

All studies mentioned above have been done on oligo- and polynucleosomes prepared from chromatin, i.e., by nuclease digestion. The reconstitution of nucleosomes from purified histones and DNA fragments of defined sequence opened the possibility of more precise observations. High-resolution X-ray diffraction studies of crystallized core particles (*4*) yielded atomic detail resolution of the structure of the histone core and the DNA in direct contact with it. Only 121 bp out of 146 were found to be in strong contact with the histone octamer. The 10 terminal base pairs on each end continue tangential to the core, in parallel planes; if the linkers would continue in the same direction, they should cross in the entry−exit region. However, electron microscopy studies on mononucleosomes (*15*) did not show a crossing of the linker DNA arms, rather a bending away from the octamer in the absence of linker histones, increased wrapping

* Corresponding author. E-mail: kati.toth@dkfz.de. Phone: 49-6221-423390. Fax: 49-6221-423391.

in the presence of the globular part of the linker histones, and a 30 bp long stem in the presence of linker histones. Cryoelectron microscopic images on mononucleosomes (*16*) with long (256 bp) linker DNA and without linker histone show the linker DNAs being slightly nonplanar, not crossing, but bending outward with a lateral divergence of $32 \pm 20°$. This study also revealed an important feature of the reconstitution, namely, that the positioning about the center of the "positioning" sequences is not unique. The "noncrossing" and "stem motif" is not a specialty of the open-ended reconstituted mononucleosomes. Cryoelectron microscopic observations on isolated oligonucleosomes (*13*) agree with this view: linker DNAs do not seem to cross, diverge without linker histones, and form a stem motif if linker histones are attached.

To complement the existing data, it would be desirable to get some direct information on the geometry of the linker DNA around the nucleosome free in solution. Such information can be obtained through intramolecular distance measurements using fluorescence resonance energy transfer (FRET).[1] Fluorescence excitation energy can be transferred from a donor to an acceptor fluorophore when the donor emission and acceptor excitation spectra overlap; this process leads to increased emission of the acceptor and quenching of the donor fluorescence (*17*). FRET is strongly distance dependent; its efficiency depends on the inverse sixth power of the distance R between the fluorophores. Therefore, FRET has been used in many fields of structural biophysics as a "molecular ruler" (*18*). We have recently measured the salt dependence of sequence-induced DNA curvature using FRET over distances on the 10 nm scale, using fluorescein as the donor and rhodamine-X as the acceptor (*19*).

The goal of the work described here is to measure the distance between the ends of DNA fragments onto which a nucleosome has been reconstituted. If the nucleosome is placed in the center of the DNA by means of a positioning sequence, the distance between the free linker DNA ends for different DNA fragment lengths will contain information about the path of the linker DNA in the mononucleosome. Since the expected distances for DNA fragments between 150 and 220 base pairs are in the range of $5-10$ nm, they can be measured by FRET. We have therefore constructed a series of DNA fragments by preparative PCR that were labeled with fluorescein or Alexa 488 on one end and with rhodamine-X on the other, reconstituted them by salt dialysis into nucleosomes, and measured the FRET as a function of fragment length. The resulting DNA length dependence of the energy transfer allows us to propose a plausible model for the path of the linker DNA outside the nucleosome. The effect of incorporation of linker histone H1 was also investigated.

MATERIALS AND METHODS

DNA Fragments. DNA fragments of different lengths ($150-220$ bp) containing the nucleosome positioning se-

quence of the *Xenopus borealis* 5S ribosomal RNA gene in the center were prepared by PCR amplification (template kindly provided by S. Dimitrov, Grenoble). The primers (INTERACTIVA GmbH, Germany) were labeled through a C_6 carbon linker with rhodamine-X or with fluorescein on their 5′ end. The donor/acceptor pair fluorescein/rhodamine-X was selected because of its high Förster radius [$R_0 = 59.6$ Å (*20*)]. Fluorescein was present as a single 5-isomer, and rhodamine-X was a mixture of the 5- and 6-isomers (Molecular Probes). The nucleotide base environment of the fluorophores was chosen to be similar, to minimize differences due to interactions with the DNA. This resulted in some cases in a $1-3$ bp asymmetry around the center of the gene. The PCR products were HPLC-purified (ion-exchange column Gen-Pak FAX, Waters) until they showed only one band on a polyacrylamide gel, either by ethidium staining or by direct fluorescence of the label. After buffer exchange on a NAP-5 column (Pharmacia, Germany), fragments were concentrated to $0.1-0.5$ mg/mL in a vacuum centrifuge (Uniequip, Germany) and stored at 4 °C in TE buffer (10 mM Tris, pH 7.5, 0.1 mM EDTA) containing 5 mM NaCl. Nonlabeled and single-labeled DNAs of the same sequence were prepared similarly. In some cases we made comparisons using Alexa 488 dye instead of the fluorescein; those primers were purchased from Genset SA, France.

Histones. Core histones (H2A, H2B, H3, and H4) were isolated from HeLa cell nuclei in nonacidic conditions in order to conserve the conformation of the histones.

HeLa cells were washed with 50 mL of PBS buffer (1.15 g of Na_2HPO_4, 0.2 g of $KHPO_4$, 8 g of NaCl, and 0.2 g of KCl per liter; final pH 7.4) and then centrifuged at 4000 rpm for 20 min. The pellet was resuspended in 20 times its own volume of lysis buffer (10 mM Tris·HCl, pH 8, 3 mM $MgCl_2$, 0.25 M sucrose, 1% NP-40, 0.5 mM PMSF) and homogenized by eight strokes in a type B pestle. After homogenization, DNA and nonhistone proteins were eliminated by washing in phosphate buffers of increasing salt concentration between 0 and 0.6 M NaCl. The last suspension in MSB buffer (50 mM sodium phosphate, pH 6.8, 0.6 M NaCl, 0.5 mM PMSF) was slowly mixed with 5 g of fast-flow hydroxylapatite (Fluka, Germany) suspended in 50 mL of MSB, then transferred into a column, and washed with another 100 mL of MSB, and the core histones were eluted with HSB buffer (50 mM sodium phosphate, pH 6.8, 2.5 M NaCl, 0.5 mM PMSF). After the buffer was exchanged into TE via dialysis, samples were concentrated and further purified on a Sepharose column (SP fast-flow, Pharmacia, Germany), eluted at 2 M NaCl. Aliquots of core histones were stored at -80 °C in TE buffer containing 2 M NaCl and 0.5 mM PMSF.

Histone H1 was purchased from Roche Diagnostics (Mannheim, Germany) and used after purification on Sepharose and a NAP-5 column. Aliquots of histone H1 were stored at -80 °C in TE buffer containing 5 mM NaCl and 0.5 mM PMSF.

The quality of the histone preparations (molecular weights and relative amounts) was controlled on a silver-stained 18% SDS−polyacrylamide gel. Comparison with nucleosomes isolated from natural chromatin (COS-7 cells) showed that in our preparation all histones were present in equimolar concentrations, without degradation.

---

[1] Abbreviations: FRET, fluorescence resonance energy transfer; spFRET, single pair fluorescence resonance energy transfer; bp, base pair; Tris, Tris(hydroxymethyl)aminomethane; EDTA, ethylenedinitrilotetraacetic acid; OD, optical density; SDS, sodium dodecyl sulfate; PAGE, polyacrylamide gel electrophoresis; MNase, micrococcal nuclease; PCR, polymerase chain reaction; PMSF, phenylmethanesulfonyl fluoride.

Nucleosome Reconstitution. Core histones and DNA fragments were mixed in TE buffer at 2 M final NaCl concentration. Typical volumes were 50−100 μL; the DNA fragment concentration was 0.4 μM. The DNA/octamer proportion varied between 1:2 and 1:3, as optimized previously for every histone preparation. The mixture stayed 30 min in silanized sterile Eppendorf tubes at room temperature; then it was transferred into collodium dialysis tubes (Sartorius, Germany) and dialyzed slowly at 4 °C against stepwise decreasing concentrations of NaCl down to 5 mM. If H1 was to be incorporated, it was added at 0.6 M NaCl concentration. Collodium was chosen as the dialysis tube material because of its chemical purity: all other tubes and membranes tested gave off optically disturbing impurities during dialysis. To decrease the loss due to adhesion, collodium tubes were extensively rinsed with core histone solution before the reconstitution. The sample volume usually increased by about 30% by the end of the dialysis.

The quality of the reconstitution was checked with gel electrophoresis either on 8% polyacrylamide gels (60:1 acrylamide:bisacrylamide) in TBE buffer at 10V/cm during 1.3 h or on 2% agarose gels in 0.5 × TBE buffer at 10 V/cm during 2 h. Gels were stained by ethidium, and a video image was taken on an UV transilluminator. The video images were quantified using the program IQ (Bio Image, USA), taking into account that the emission of ethidium is about 30% weaker in the case of nucleosomes than for free DNA (*21*). To demonstrate the incorporation of H1 linker histone, we looked for the slowing down of the migration of nucleosomes in agarose gels and also made MNase digestion tests. MNase (Roche Diagnostics, Mannheim, Germany) was added at 5 units/mL to the nucleosome solutions. Digestion by MNase was done in the presence of 1 mM $CaCl_2$ for different incubation times at 25 °C and was stopped by EDTA. The samples were analyzed on 8% PAGE (29:1) after phenolization.

Absorption and Emission Spectra. For all measurements the samples were thermostated at 20 °C. Quartz cuvettes with a path length of 3 mm were used. Cuvettes were silanized in order to avoid adhesion of the dye or proteins. Low sample concentrations were used to avoid inner filter effects in the fluorescence measurements. Absorbances at the dye absorption maxima were held below 0.01, corresponding to dye concentrations below 450 nM.

Absorption spectra were measured on a Cary 4E spectrometer (Varian, Mulgrave, Australia) between 220 and 750 nm, with an OD accuracy of 0.001. Emission spectra were measured with an SLM-AMINCO 8100 fluorescence spectrometer (SLM, Urbana, IL) using a 150 W xenon lamp. Emission spectra were collected between 500 and 750 nm with a 4 nm monochromator slit width for excitation and emission. Excitation wavelengths were 495 nm for the donor and 585 nm for the acceptor. Spectra were measured relative to the lamp intensity and corrected for the instrument response and buffer signal. To correct for concentration differences, spectra were normalized at the emission maximum of the donor. Numerical treatment of the collected data was done with the program Kaleidagraph on a Macintosh computer. For the determination of the energy transfer efficiency, integrated spectral regions were used: the integration extended over ±5 nm in the absorption spectra and ±10 nm in the emission spectra.

RESULTS AND DISCUSSION

Characterization of the Reconstituted Nucleosomes. During the reconstitution of the nucleosomes, one unavoidably obtains byproducts such as free DNA, aggregates, and incompletely wound nucleosomes, which are hard to separate from the mononucleosomes without degrading them. We therefore made an effort to optimize the production of correctly reconstituted nucleosomes and to quantitate the other products.

Free DNA will produce an additional fluorescence donor signal but no energy transfer because of the big distance (>50 nm) between the donor and acceptor. The amount of free DNA in the preparation was therefore quantitated from gels as described in the Materials and Methods section. The relationship between total integrated area under a fluorescent spot and amount of DNA was calibrated using a concentration series with an internal standard (data not shown). For further experiments, we used only samples where the free DNA was below 10% (Figure 1a).

Aggregation, which produces interparticle FRET, had to be minimized in the preparations. Indications of aggregation are a sloping baseline in the absorption spectrum or a pronounced Rayleigh scattering peak in the fluorescence emission spectrum. We used only samples where the difference in absorbance between 650 and 400 nm (the flat parts of the spectrum) was less than 0.002 absorbance unit and where the scattering peak in the emission spectrum was not significantly higher than for the case of free DNA (data not shown). If necessary, aggregates were separated by airfuge centrifugation.

A reconstituted nucleosome sample, even on a positioning sequence, consists of a population of nucleosomes of different mobility on polyacrylamide gels. We aimed to compare samples with a similar distribution of positioning; therefore, we characterized all preparations by native polyacrylamide gel electrophoresis (Figure 1b). In some preparations we observed nucleosomes that exhibited a significantly higher mobility in agarose gels. These bands have been assigned to nucleosomes with incomplete histone cores (*22*) and have to be avoided in the FRET measurements; thus, the sample was always cross-checked against isolated COS-7 mononucleosomes by agarose gel electrophoresis (Figure 1a).

The relative amount and integrity of the incorporated histones in the nucleosomes were controlled by SDS−PAGE (Figure 1c) after extraction of the corresponding bands from native polyacrylamide gels. We could observe no degradation and the same proportions between the core histones as in the COS-7 mononucleosomes. The linker histones could not be quantified by this method, due to the increased background in the presence of the dyes.

Absorption and emission spectra have shown no qualitative difference between single-labeled fragments and nucleosomes. This indicates that the environment of the dyes is not perturbed by the presence of the octamers, even for the shortest 150 bp fragments.

These controls enabled us to perform the fluorescence measurements on samples containing nucleosomes with similar distribution of positioning, less than 10% free DNA without aggregates.

Distance Measurements. The energy transfer was measured through the enhanced emission of the acceptor. Spectral data
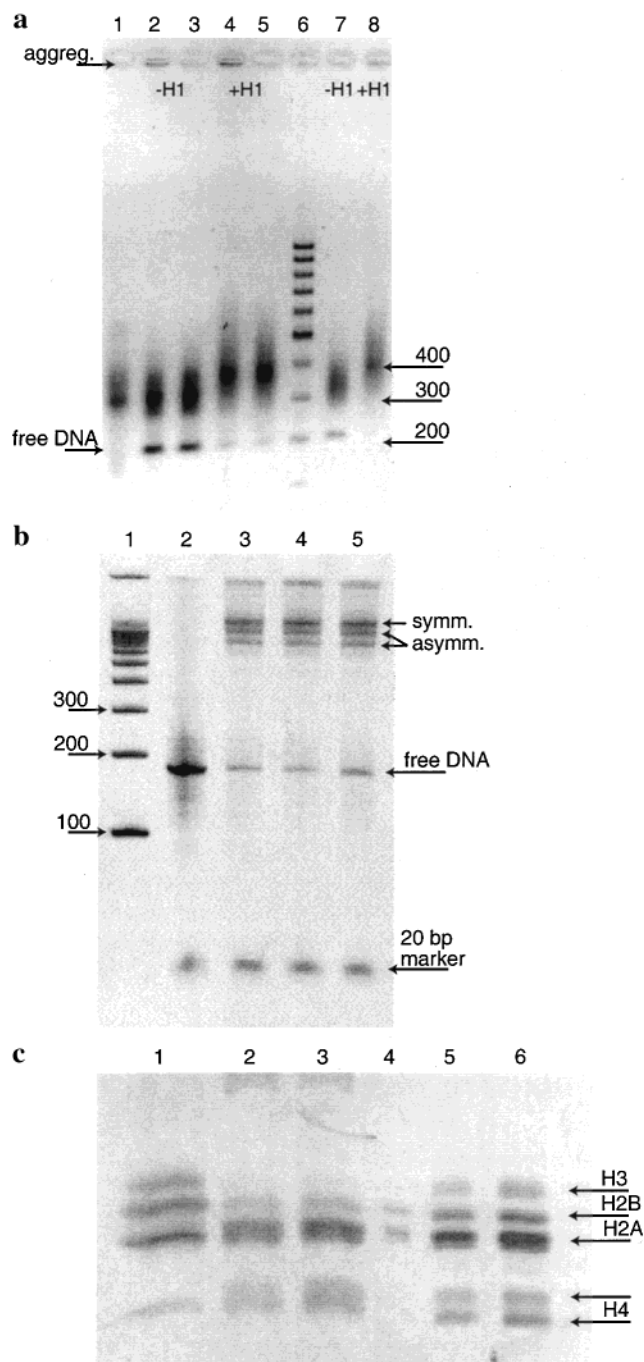
FIGURE 1: Characterization of reconstituted mononucleosomes by gel electrophoresis. (a) Determination of the ratio of nucleosomes to free DNA and control of the integrity of the nucleosomes on agarose gel. Lanes: 1, nucleosomes isolated from COS-7 cells; 2−5, nucleosomes reconstituted with 190 bp DNA double labeled with Alexa 488 and rhodamine-X; 6, DNA marker; 7 and 8, nucleosomes reconstituted from nonlabeled 203 bp DNA. Samples in lanes 2 and 4 contain aggregates as seen in the loading well of the gel. Samples in lanes 3 and 5 were taken after centrifugation. The decreased mobility in lanes 4, 5, and 8 shows the incorporation of H1 linker histone. (b) Comparison of positioning distribution by PAGE of nucleosomes reconstituted from 182 bp DNA double labeled with fluorescein and rhodamine-X. Lanes: 1, DNA marker; 2, free DNA; 3−5, nucleosomes prepared in three different assays. Lanes 2−5 contain equal concentrations of a short oligonucleotide for quantification. (c) Control of the histone composition of nucleosomes reconstituted from 203 bp nonlabeled DNA excised from PA gel and analyzed on SDS−PAGE. Lanes: 1, nucleosomes isolated from COS-7 cells; 2 and 3, reconstituted nucleosomes at 0.1 and 5 mM NaCl, respectively; 4−6, mixture of core histones in increasing amounts, 0.25, 0.5, and 0.75 μg, respectively.
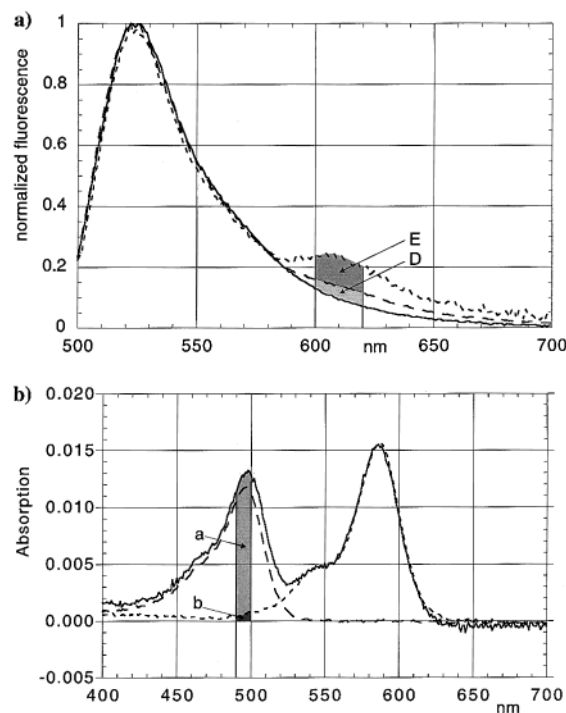

FIGURE 2: Spectra used in the calculation of energy transfer using fluorescein as donor and rhodamine-X as acceptor on 182 bp DNA. (a) Normalized emission spectra of donor-only labeled DNA (−), double-labeled DNA (---), and double-labeled nucleosome (···). The excitation wavelength was 495 nm. E and D are the integrated areas corresponding to the enhanced emission and direct excitation of the acceptor. (b) Absorption spectra of donor-only (---), acceptor-only (···), and double-labeled DNA (−), normalized to the DNA absorption peak. a and b are the integrated areas corresponding to the absorption at the donor excitation wavelength of the donor and acceptor in the double-labeled sample.

of three emission spectra and two absorption spectra had to be taken into account in the calculation (Figure 2). The measured emission spectra were corrected for the instrument response, and the signal of the buffer was subtracted. Then the emission spectra of the donor-only labeled fragment, the double-labeled fragment, and the double-labeled nucleosomes were normalized at the emission maximum of the donor. These spectra coincide perfectly in the 500−570 nm region. Normalization was necessary to account for concentration differences. For the same reason, measurements on the donor side would also be too difficult. To calculate the enhanced emission, we used the integrated spectral area between 600 and 620 nm. The enhanced acceptor emission is characterized by the difference of the double-labeled nucleosome and fragment (E), while the acceptor emission due to direct excitation (D) is the difference between the double-labeled and donor-only labeled fragment. The energy transfer ET is calculated as their proportion corrected by the absorption of the donor (a) and the acceptor (b) in the double-labeled nucleosome at the donor excitation wavelength (495 nm):

$$ET = \frac{E/a}{D/b} \qquad (1)$$

The tail of the acceptor absorption at 495 nm (Figure 2b) was calculated from the absorption spectra of the acceptor-only labeled fragment. The proportion of the absorption at its maximum (585 nm) and at 495 nm was determined (20 ± 1), and this value was used for the double-labeled samples.

To increase the precision, these absorption spectra were recorded at relatively high DNA concentrations [OD (at 585 nm) >0.01], and integration of ±5 nm around the maxima was applied. The proportion of the absorption of the acceptor-only labeled fragment at 585 and 495 nm was also controlled by fluorescence measurements: the corrected emissions due to excitation at these wavelengths gave the same proportion.

The precision of the determination of the different correction terms (a, b, D) was better than 5%, and they indicated no relative difference between the samples. The quantity E depends on the average distance of the dyes and will thus vary according to fragment length. However, due to varying percentages of free DNA and to differences in the positioning and completeness of nucleosome formation, a higher variability was observed for repetitive preparations of the samples. The effect of free DNA was minimized by using only data from samples with less than 10% of free DNA, and the ET value was corrected for this percentage. We estimate the error due to this correction to be less than 2% of the ET values. The positioning and completeness of the nucleosomes were compared on gel images: we used only those samples whose mobility on an agarose gel was not higher than that of the control COS-7 sample and which contained the correct proportion of core histones as verified on a polyacrylamide gel.

In the calculation of the dye-to-dye-distances, the Förster distance R_0 of the two dyes is defined as

$$R = R_0(1/\text{ET} - 1)^{1/6} \qquad (2)$$

It should be kept in mind that in the averaging of FRET-determined distances relatively more weight is given to those conformations where the two dyes are closest together, because the energy transfer depends on the dye-to-dye distance in a strongly nonlinear fashion. Thus, in a population of nucleosomes with different positioning, symmetrically positioned nucleosomes are weighted more strongly because here the linker ends are closer together. Also, when the dyes can move with respect to one another because of flexibility of the linker connecting the dye to the DNA or of the DNA itself, short distances will be weighted relatively stronger.

For the fluorescein/rhodamine-X pair we used the distance 59.6 Å that was published earlier (20) and found satisfactory in our previous study (19). For the Alexa 488/rhodamine-X pair we calculated R_0 relative to the fluorescein/rhodamine-X pair, taking into account the differences in the emission spectra of the two donors and their quantum yields. We obtained a value of 55 ± 0.5 Å. On the basis of earlier measurements on the anisotropy of these dyes linked through a C_6 chain to the DNA, we could use an anisotropy factor $\kappa = \frac{2}{3}$ in both cases. Due to the sixth power dependence of R on ET, the errors in the calculated distance will be largely reduced: the scaling error, estimated to be less than 5% in ET, results in an error of only 1−2% in the distance between 60 and 90 Å. At shorter distances, the error is even less.

In summary, the estimated upper limit for the errors is the following: the systematic error is less than 2%, and errors introduced by the estimate of free DNA is also less than 2%. The standard deviation of the determined distances was between 2 and 4%, and a distance underestimation takes place due to the weighted averaging. However, as mentioned
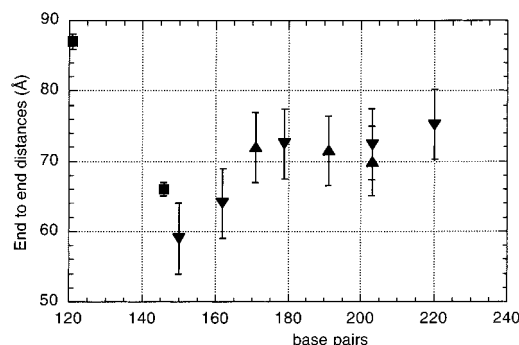

FIGURE 3: Dependence of the end-to-end distance of the nucleosomal DNA on the fragment length. Data points were calculated from FRET measurements using fluorescein (▼) or Alexa488 (▲) as donor. Two points are added which are calculated from the published crystal structure (■) (4).

above, this weighting will prefer the symmetrically positioned nucleosomes to the asymmetric ones.

Path of the Linker DNA. We have determined the averaged dye-to-dye distances from the FRET measurements in dependence of the DNA length. We assume that the dyes have the same freedom to rotate around the DNA ends for every fragment. On the basis of earlier assumptions (19), the identification of the dye-to-dye distance with the end-to-end distance will not affect the relative differences between fragments, and the absolute distance error is less than 5%. Figure 3 shows the results together with two points calculated from the published crystal structure (4). At 121 bp—the last bases bound tightly to the histone core—the distance between the centers of the helix is 87 Å. Assuming a tangential path for the last 10 base pairs as proposed in the crystal structure, at 145 bp this distance is 66 Å. This last value agrees quite well with the measured distance (60 ± 5 Å) for the nucleosome reconstituted on the 150 bp fragment. The distances show a slight but definite increase from about 60 ± 5 to 75 ± 5 Å between 150 and 170 base pairs and stabilize above that length. Measurements using Alexa 488 as a donor yielded the same distances as with the fluorescein donor, within experimental error.

(A) Straight, Rigid Linker DNA. Restricting ourselves first to the hypothetical case that the linker DNA arms outside the core are straight and rigid, we shall try to distinguish between geometries compatible and noncompatible with our FRET data. Schematic views of possible geometries in two projections are given as illustrations in Figures 4 and 5. We defined the direction of the superhelical axis of the histone octamer as vertical and the plane perpendicular to it as horizontal.

If we assume that the linker DNA strands leaving the nucleosome continue in a straight line following the direction of the last helix turn in the crystal structure, i.e., leaving tangentially in the horizontal plane and continuing the slope of the superhelix vertically, the three-dimensional distance would have a minimum at around 170−180 base pairs (Figure 4a). However, our data present no minima over the whole range. If we conserve just the horizontal path as tangential and fit the vertical distances to the measured FRET results, a nonmonotonous vertical path arises, which cannot be explained within the limit of a straight, rigid linker DNA.

(B) Kinks in the Path of the Linker DNA. Cryoelectron microscopy images suggest a slight outward divergence of
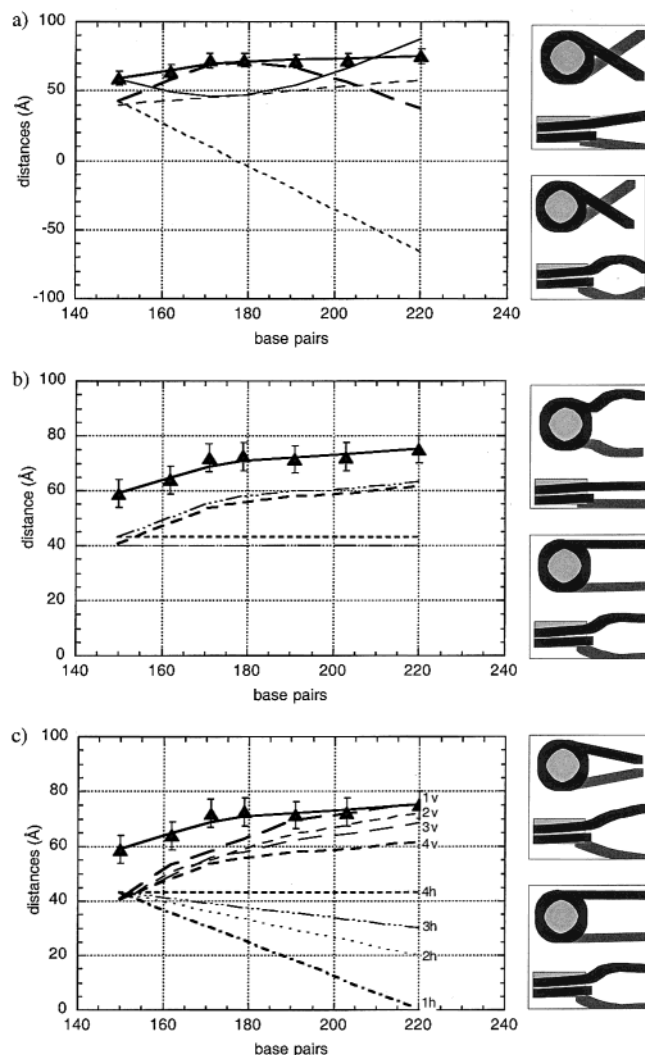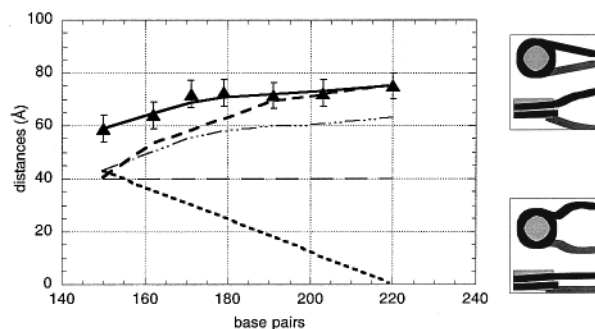
FIGURE 5: Range of the trajectories compatible with the measured distances. The extreme paths are taken from Figure 4b,c. The vertical distances of the extremes are (− −) and (---); the corresponding horizontal distances are (···) and (− ··· −).

recently by mapping the frequency of pyrimidine dimer formation (*23*).

Intermediates between the two special cases of constant vertical or horizontal distance might also be compatible with the FRET measurements, if no crossing is allowed up to the maximum measured length of 220 bp (Figure 4c). If we allow a kink of the DNA axis at the exit points, but not farther away from the core, we can define the geometrical limits of the possible linker path, varying from slightly approaching to slightly diverging in the horizontal and from parallel to diverging in the vertical direction. Figure 5 shows these two limiting geometries. Thus, our results suggest that in free solution the linker DNAs tend to diverge and do not cross, in agreement with the EM observations referred to above.

The distances were presented above as a function of the number of base pairs. We may calculate possible opening angles between the linker DNAs by taking into account the extremes presented in Figure 5 and defining the approximate linear distance from the core, L, as $L = 3.4 \ \text{Å} \times$ (DNA length in bp − 150 bp)/2. We obtain a maximum opening angle of 20° (±10°) vertically (for the first extreme) or 26° (±10°) horizontally (in the second extreme). These values are compatible with cryo-EM observations on mononucleosomes (*16*) but lower than those determined on chromatin fragments (*12*, *13*) and by other microscopic methods (*14*). In general, all distances measured in Figure 3 are smaller than the diameter of the nucleosome itself, a behavior that is rarely seen in microscopic images. This difference may be explained by the flexibility of the DNA (see below); on the other hand, differences from the solution structure may also occur from interaction with the support necessary for microscopy or due to fixation. Another difference to consider is that some microscopic observations were done in the presence of Mg^{2+} (*15*); this, however, is expected to decrease rather than increase the opening angle. On the other hand, our own preliminary FRET data (not shown) show that increasing the salt concentration across the range where the nucleosomes conserve their integrity has rather little effect on the end-to-end distance.

(C) Effect of Linker DNA Flexibility or Curvature. In Figure 3, the plot of linker end-to-end distance vs DNA fragment length increases monotonically with a negative curvature. From the argumentation given above, one can conclude that this behavior is not compatible with rigid linker DNA ends extending from the nucleosome core in straight lines. In general, the distance between the ends of two straight line segments that extend in length by the same amount along

FIGURE 4: Vertical and horizontal components of the end-to-end distances of the linker DNA ends calculated under different assumptions and related to the measured distances (▲). (a) Assumption: The DNA leaves the core tangentially in the horizontal direction (···). Resulting end-to-end distance has a minimum around 180 bp (—) if the vertical path (---) is also continued without change. Fitting the measured end-to-end distances requires a nonmonotonic vertical path (− −). (b) Assumption: Constant distance in one of the projections and fit to the measured values in the other; fixed vertical spacing of 40 Å (---) and corresponding horizontal opening (− ··· −) or fixed horizontal spacing of 43 Å (···) and corresponding vertical opening (− −). (c) Assumption: no kinks far from the core; straight horizontal path (1−4h) in different directions and corresponding vertical distances fit to the measured values (1−4v).

the linker DNA arms in the absence of H1 both in reconstituted mononucleosomes (*15*) and in chromatin fiber fragments (*13*): in some projections the linker DNAs are parallel. If we fix the horizontal or the vertical distance as constant and fit the other to the FRET results (Figure 4b), a divergence in these directions can be seen. For a fixed horizontal spacing, the vertical distance will diverge more strongly than expected from the pitch of the nucleosomal superhelix alone. On the other hand, if we keep the vertical distance constant, the horizontal path will contain a strong kink outward from the core. Both of these changes of direction might be possibly explained by an interaction with part of the histones, so we cannot exclude them. Evidence for kinks at the exit points of the linker DNA was presented

their original direction can decrease down to a minimum and then increase again. Therefore, it may exhibit a positive but never a negative curvature (this can easily be shown by simply taking two points on two separate straight lines in vector notation, $\vec{r}_1(\lambda) = \vec{R}_1 + \lambda \vec{e}_1$, $\vec{r}_2(\lambda) = \vec{R}_2 + \lambda \vec{e}_2$, and differentiating their distance twice with respect to λ).

Thus, a straight trajectory of the free linker DNA ends beyond the nucleosome core is quite unlikely. One explanation could be that the linker DNA exhibits some kind of curvature that extends outside the superhelical part of the nucleosome; it has been suggested that superhelicity might induce long-range structural changes in DNA (*24*). Alternatively, since the linker DNA is *not* completely rigid, the distance between the two ends will fluctuate; as explained above, the R^{-6} dependence of FRET on the distance will give a greater weight to short distances. With increasing DNA length, the amplitude of elastic excursions of the linker DNA ends about their equilibrium position will increase, and therefore the FRET-observed distance will be smaller than the linear average. Thus, both DNA bending and DNA flexibility could give rise to the negative curvature observed in Figure 3.

Information about the distance distribution function between the chromophores in a FRET experiment can in principle be obtained by methods that do not only analyze the average energy transfer efficiency but separate the contributions of individual members in a distribution of conformations. One possibility would be to analyze the distribution of donor fluorescence lifetimes by a multiexponential decomposition technique; for lack of a suitable instrument, this route could not be taken here. Another technique that has very recently been introduced is single pair FRET (spFRET), where the FRET efficiencies of individual molecules are analyzed separately and a histogram of FRET efficiencies is obtained directly (*25*). Studies of the FRET distribution on reconstituted nucleosomes by spFRET are in progress in our group.

Incorporation of Linker Histone H1 Pulls the Linker DNAs Closer. FRET measurements were also done on nucleosomes containing H1 histones. Binding of the linker histone to the nucleosome results in a decrease of its mobility in agarose gel electrophoresis (Figure 1a). The correct incorporation of the linker histone could be shown qualitatively by micrococcal nuclease digestion: we found a stop near 170 bp, very similar to the one that is found when H1-containing native nucleosomes are digested (Figure 6). This stop was not found when H1 was absent. An upper limit of the H1/nucleosome ratio was estimated from the spectrophotometrically determined amount of the nucleosomes after the reconstitution and the added amount of H1 histones. Because of the possibility of H1 adhesion on the dialysis tube and of the presence of nonbound linker histones, this may be an overestimation.

Figure 7 shows the change in the normalized fluorescence emission curves of nucleosomes with increasing amounts of added H1: the linker histone per nucleosome ratio is estimated to be 0.68 in the first case and 1 in the second. The enhanced emission of the acceptor increased with increasing H1. The calculated energy transfer values increased by 9% and 19% ($\pm 2\%$) for the two different H1 stoichiometries. This reflects a change in the relative population of nucleosomes with and without linker histone and would formally
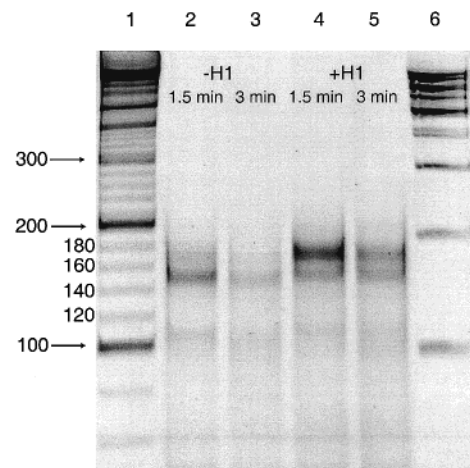

FIGURE 6: Demonstration of the incorporation of linker histone H1 in the nucleosomes reconstituted from 191 bp double-labeled DNA through the stop in MNase digestion visualized by PAGE. Lanes: 1 and 6, DNA marker; 2 and 3, nucleosomes without H1; 4 and 5, nucleosomes with H1.
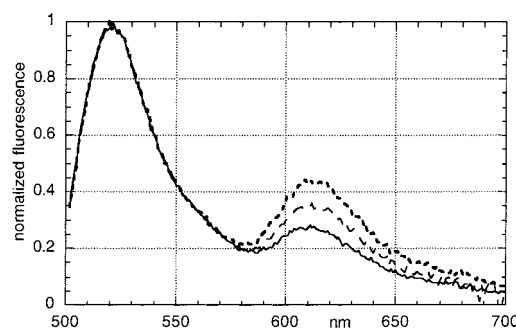

FIGURE 7: Effect of increasing H1 incorporation on the energy transfer. Normalized fluorescence emission curves of nucleosomes reconstituted from 191 bp double-labeled DNA without H1 (—), with H1/NS = 0.68 (---), and with H1/NS = 1.00 (···). The excitation wavelength was 495 nm.

correspond to a decrease in the average distance of 6 and 10 Å (± 2 Å), respectively. We assume that the latter value is probably a lower limit of the distance change caused on one nucleosome by H1 binding. The approach of the linker DNA ends of about 5–10 Å at approximately 1 added H1 per nucleosome was found at all DNA lengths examined. The uncertainty in the determination of the H1 binding stoichiometry did not allow us to make a precise quantitative comparison for the effect of H1 at different DNA lengths. However, we found no indication for crossing of the linkers even in the presence of linker histones for DNA fragment lengths up to 220 bp. While we cannot exclude wrapping of the linker DNA arms around each other under the influence of H1, this result in solution is compatible to the formation of the stem motif observed earlier in fixed EM preparations of mononucleosomes (*15*) and in cryo-EM images of polynucleosomes (*13*).

FRET distance measurements at saturated H1/nucleosome ratios were impossible since we found that more elevated concentrations of H1 led to aggregation, rendering the data unusable. As mentioned above, such aggregation was visible in the absorption spectrum and in the Rayleigh scattering peak of the fluorescence emission spectrum. We note that incorporation of H1 by dialysis seems to be essential for obtaining the maximum effect; simple addition of H1 to a

solution of labeled nucleosomes at 5 or 50 mM NaCl showed an increase in FRET that was much smaller than in the dialyzed samples (data not shown).

The role of the linker histones in the proper organization of the chromatin fiber and their location has been discussed since their discovery (for recent reviews, see refs *6* and *26−28*). A consensus seems to exist that linker histones and appropriate ionic conditions are co-responsible for the formation and stability of a compact 30 nm fiber, both acting through charge neutralization of the linker DNA. The linker histone induced distance decrease between the linker DNA arms that we observe here is in agreement with this view.

The results above characterize the geometry of linker DNA with free ends on mononucleosomes, without internucleosomal interactions. Such interactions between histone octamers, histone tails, and linker DNA, or effects due to the attachment of DNA ends on consecutive core particles, should now be investigated by complementary methods.

ACKNOWLEDGMENT

REFERENCES

1. Olins, A. L., and Olins, D. E. (1974) *Science 183*, 330−332.
2. Kornberg, R. D. (1974) *Science 184*, 868−871.
3. Arents, G., Burlingame, R. W., Wang, B.-C., Love, W. E., and Moudrianakis, E. N. (1991) *Proc. Natl. Acad. Sci. U.S.A. 88*, 10148−10152.
4. Luger, K., Mäder, A. W., Richmond, R. K., Sargent, D. F., and Richmond, T. J. (1997) *Nature 389*, 251−260.
5. Finch, J. T., and Klug, A. (1976) *Proc. Natl. Acad. Sci. U.S.A. 73*, 1897−1901.
6. van Holde, K., and Zlatanova, J. (1996) *Proc. Natl. Acad. Sci. U.S.A. 93*, 10548−10555.
7. Woodcock, C. L., Grigoryev, S. A., Horowitz, R. A., and Whitaker, N. (1993) *Proc. Natl. Acad. Sci. U.S.A. 90*, 9021−9025.
8. Prunell, A. (1998) *Biophys. J. 74*, 2531−2544.
9. Butler, P. J., and Thomas, J. O. (1998) *J. Mol. Biol. 281*, 401−407.
10. Yao, J., Lowary, P. T., and Widom, J. (1990) *Proc. Natl. Acad. Sci. U.S.A. 87*, 7603−7607.
11. Hammermann, M., Toth, K., Rodemer, C., Waldeck, W., May, R. P., and Langowski, J. (2000) *Biophys. J. 79*, 584−594.
12. Bednar, J., Horowitz, R. A., Dubochet, J., and Woodcock, C. L. (1995) *J. Cell Biol. 131*, 1365−1376.
13. Bednar, J., Horowitz, R. A., Grigoryev, S. A., Carruthers, L. M., Hansen, J. C., Koster, A. J., and Woodcock, C. L. (1998) *Proc. Natl. Acad. Sci. U.S.A. 95*, 14173−14178.
14. Leuba, S. H., Bustamante, C., van Holde, K., and Zlatanova, J. (1998) *Biophys. J. 74*, 2830−2839.
15. Hamiche, A., Schultz, P., Ramakrishnan, V., Oudet, P., and Prunell, A. (1996) *J. Mol. Biol. 257*, 30−42.
16. Furrer, P., Bednar, J., Dubochet, J., Hamiche, A., and Prunell, A. (1995) *J. Struct. Biol. 114*, 177−183.
17. Förster, T. (1946) *Naturwissenschaften 6*, 166−175.
18. Clegg, R. M. (1996) in *Fluorescence imaging spectroscopy and microscopy* (Wang, X. F., and Herman, B., Eds.) pp 179−252, John Wiley & Sons, New York.
19. Tóth, K., Sauermann, V., and Langowski, J. (1998) *Biochemistry 37*, 8173−8179.
20. Parkhurst, K. M., and Parkhurst, L. J. (1995) *Biochemistry 34*, 293−300.
21. McMurray, C. T., Small, E. W., and van Holde, K. E. (1991) *Biochemistry 30*, 5644−5652.
22. Hayes, J. J., and Lee, K. M. (1997) *Methods 12*, 2−9.
23. Pehrson, J. R., Litwin, S., Myers, C. B., and Cohen, L. H. (1999) *Methods 19*, 447−456.
24. Schurr, J. M., Delrow, J. J., Fujimoto, B. S., and Benight, A. S. (1997) *Biopolymers 44*, 283−308.
25. Deniz, A. A., Dahan, M., Grunwell, J. R., Ha, T., Faulhaber, A. E., Chemla, D. S., Weiss, S., and Schultz, P. G. (1999) *Proc. Natl. Acad. Sci. U.S.A. 96*, 3670−3675.
26. Carruthers, L. M., Bednar, J., Woodcock, C. L., and Hansen, J. C. (1998) *Biochemistry 37*, 14776−14787.
27. Widom, J. (1998) *Curr. Biol. 8*, R788−R791.
28. Travers, A. (1999) *Trends Biochem. Sci. 24*, 4−7.